

Two-way Node Popularity Model for Directed and Bipartite Networks

Bing-Yi Jing

JINGBY@SUSTECH.EDU.CN

*Department of Statistics and Data Science
Southern University of Science and Technology
Shenzhen 518055, China*

Ting Li

TINGERIC.LI@POLYU.EDU.HK

*Department of Applied Mathematics
The Hong Kong Polytechnic University
Hong Kong 999077, China*

Jiangzhou Wang

WANGJZ695@SZU.EDU.CN

*School of Mathematical Sciences, Institute of Statistical Sciences
Shenzhen University
Shenzhen 518060, China*

Ya Wang

WANGYA@SUSTECH.EDU.CN

*Department of Statistics and Data Science
Southern University of Science and Technology
Shenzhen 518055, China*

Abstract

There has been extensive research on community detection in directed and bipartite networks. However, these studies often fail to consider the popularity of nodes in different communities, which is a common phenomenon in real-world networks. To address this issue, we propose a new probabilistic framework called the Two-Way Node Popularity Model (TNPM). The TNPM also accommodates edges from different distributions within a general sub-Gaussian family. We introduce the Delete-One-Method (DOM) for model fitting and community structure identification, and provide a comprehensive theoretical analysis with novel technical skills dealing with sub-Gaussian generalization. Additionally, we propose the Two-Stage Divided Cosine Algorithm (TSDC) to handle large-scale networks more efficiently. Our proposed methods offer multi-folded advantages in terms of estimation accuracy and computational efficiency, as demonstrated through extensive numerical studies. We apply our methods to two real-world applications, uncovering interesting findings.

Keywords: Bipartite network, Community detection, Directed network, Node popularity

1 Introduction

Community detection is a valuable tool for understanding the structure of a network and has been applied in various fields, including biology (Calderer and Kuijjer (2021); Li et al. (2021)), social science (Wu et al. (2020); Jing et al. (2022)), and global trading analysis (Jing et al. (2021)). While several models have been proposed for community detection in undirected networks, the study of community detection in directed and bipartite networks is relatively limited.

One reason is that directed networks are more complex than undirected ones as they involve both outgoing and incoming links. Therefore, traditional definitions of clustering problems, such as intra-cluster and inter-cluster edge density, cannot be extended directly to directed networks (Zhang

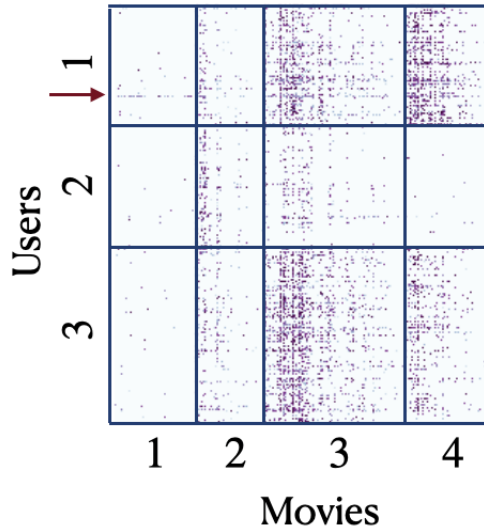


Figure 1: The adjacency matrix of MovieLens 100K Data set is rearranged by the clustering results obtained through the proposed TSDC method, with blue lines marking the cluster boundaries.

et al. (2021)). Bipartite networks, on the other hand, have nodes divided into two sets and edges that only connect nodes from different sets. This feature violates the assumption of symmetric relationships between nodes in undirected scenarios.

To address this gap, several studies have been conducted. The pseudo-likelihood approach has been used to identify out- and in-community structures in Amini et al. (2013) and Wang et al. (2023). Rohe et al. (2016) proposes the Stochastic co-Blockmodel (ScBM) and its extension, the Degree Corrected ScBM (DC-ScBM), which considers degree heterogeneity to model directed networks. Wang et al. (2020) analyzes the theoretical guarantees for the algorithm D-SCORE (Ji and Jin (2016)) and its variants designed under DC-ScBM. Zhou and Amini (2019) studies spectral clustering algorithms designed by a data-driven regularization of the adjacency matrix under ScBM. In Zhang et al. (2021), authors embed nodes with concentration restrictions to help identify communities.

However, all of the above methods overlook the heterogeneous popularities of nodes across different communities. Such structure has been widely observed and discussed in undirected networks (Sengupta and Chen (2018); Noroozi et al. (2021b)). Addressing this, Sengupta and Chen (2018) proposes the Popularity Adjusted Stochastic Block Model (PABM), which models the edge probability between two nodes as a product of node popularity parameters. PABM provides a flexible way of modeling the probability of connections and allows nodes in the same community to exhibit heterogeneous popularities across different communities.

Diverse node popularity patterns are also widely present in directed or bipartite scenarios. One motivating example is the MovieLens 100K data set (Harper and Konstan (2015)), which depicts a bipartite network where entries represent user-to-movie ratings. Illustrated in Figure 1, the adjacency matrix is organized according to clustering results, with cluster boundaries marked by blue

lines. This visualization reveals that group 1 users predominantly prefer movies in categories 3 and 4, though there’s limited but notable interest in categories 1 and 2, with a few exceptions (highlighted by a red arrow) showing curiosity in category 1. Such diversity in node popularities reveals various consumer patterns and contributes to understanding the different behaviors of users with respect to movies from different categories.

Existing algorithms for undirected networks are not easily extendable to directed and bipartite scenarios. For example, the algorithm proposed in Sengupta and Chen (2018) is limited to networks with a small number of communities (less than 3). On the other hand, while the Sparse Subspace Clustering (SSC) algorithm proposed in Noroozi et al. (2021b) can handle large-scale networks, it is sensitive to noise, as demonstrated by the simulation results in Section 5. Moreover, our numerical studies indicate that naively applying these methods to directed and bipartite networks often leads to poor performance.

In this paper, we introduce the Two-Way Node Popularity Model (TNPM), a comprehensive probabilistic framework designed to model directed and bipartite networks with community structures and node popularities. Moreover, the TNPM allows each link to be generated from different distributions within the sub-Gaussian family. The new model presents significant challenges in model fitting due to the use of two distinct sets of scaling parameters to characterize node popularities for the out- and in-communities separately. Our main contributions are listed as follows:

- We propose the Two-Way Node Popularity Model (TNPM) to model directed and bipartite networks with community structures and node popularities. The model also generalizes link distributions to the sub-Gaussian family.
- To fit the model, we introduce the Delete-One-Method (DOM) with theoretical guarantees, and the Two-Stage Divided Cosine Algorithm (TSDC) for large-scale networks. Both methods have been empirically proven to be superior to state-of-the-art methods.
- We prove the consistency of the DOM under the TNPM, including the consistency of the estimated probability matrix and the detected out- and in-community structures. We adopt a new strategy to directly upper bound the operator norm of random matrices to overcome the technical issue raised by following former works, which need to prove the concentration inequality for the Lipschitz function of independent sub-Gaussian random variables.

To the best of our knowledge, this is the first systematic study of directed and bipartite networks that considers node popularities, and the study on sub-Gaussian generalization might be of independent interest.

The rest of the paper is organized as follows. Section 2 introduces the Two-Way Node Popularity Model (TNPM). In Section 3, we propose the Delete-One-Method (DOM) and the Two-Stage Divided Cosine Algorithm (TSDC). We explore the theoretical properties in Section 4. Section 5 and 6 present extensive simulations and real data applications to demonstrate the advantages of the proposed methods.

2 Two-way Node Popularity Model

Consider a bipartite network $\mathcal{G}(U, V, E)$ with two sets of nodes U and V indexed as $1, \dots, n$ and $1, \dots, m$, respectively. The directed network can be viewed as a special case of the bipartite network

when $U = V$. Therefore, from this point onward, we will solely focus on bipartite graphs, and all the algorithms and conclusions derived will also be applicable to directed networks.

Let $A = (A_{ij})_{i,j=1}^{n,m}$ denote the adjacency matrix of the network, where $A_{i,j}$ represents the weights from node i in set U to node j in set V . We use $A_{i\cdot}$ to denote the i -th row of matrix A , and $A_{\cdot j}$ to denote the j -th column of A . The community structure associated with nodes in set U is referred to as the out-community, and the community structure associated with nodes in set V is referred to as the in-community. Let K and L denote the number of out-communities and in-communities, respectively. The distinct blocks are denoted as \mathcal{N}_k and \mathcal{M}_l for all $k = 1, \dots, K$ and $l = 1, \dots, L$.

For brevity, we introduce the following notations. For any set Ω , denote cardinality of Ω by $|\Omega|$. For any numbers a and b , $a \wedge b = \min(a, b)$ and $\lfloor a \rfloor$ represents the largest integer less than or equal to a . For any integer I , denote $[I]$ as the set $\{1, 2, \dots, I\}$. We define $n_k = |\mathcal{N}_k|$ and $m_l = |\mathcal{M}_l|$ for all $k \in [K]$ and $l \in [L]$. Furthermore, let $\mathbf{c} \in \{1, 2, \dots, K\}^n \triangleq [K]^n$ and $\mathbf{z} \in \{1, 2, \dots, L\}^m \triangleq [L]^m$ represent the vectors of out-community and in-community assignments, respectively. Specifically, $c_i = k$ if and only if node i belongs to out-community \mathcal{N}_k , and $z_j = l$ if and only if node j belongs to in-community \mathcal{M}_l . Denote $\mathcal{M}_{n,K}$ and $\mathcal{M}_{m,L}$ as the collections of clustering matrices $C \in \{0, 1\}^{n \times K}$ and $Z \in \{0, 1\}^{m \times L}$, respectively, where $C_{ik} = 1$ if $i \in \mathcal{N}_k$ and $Z_{jl} = 1$ if $j \in \mathcal{M}_l$.

To model the popularity of nodes in rows and columns separately, we propose a Two-Way Node Popularity Model (TNPM):

$$P_{ij} = \mathbb{E}(A_{ij}) = \Lambda_{i\mathbf{z}_j} \tilde{\Lambda}_j \mathbf{c}_i, \quad (1)$$

where Λ_{il} , $1 \leq i \leq n$, $1 \leq l \leq L$, and $\tilde{\Lambda}_{jk}$, $1 \leq j \leq m$, $1 \leq k \leq K$ are the node popularity parameters. Λ_{il} describes the popularity of node i among the in-community \mathcal{M}_l , while $\tilde{\Lambda}_{jk}$ represents the popularity of node j among the out-community \mathcal{N}_k .

Additionally, given \mathbf{c} and \mathbf{z} , the A_{ij} 's are assumed to be mutually independent and follow a sub-Gaussian distribution with $\mathbb{E}(A_{ij}) = P_{ij}$, such as Bernoulli, Binomial and Normal distribution. It is crucial for modeling real data, since there is no prior knowledge of specific distributions.

The mean structure of the adjacency matrix A under TNPM exhibits a block rank-one structure, which constitutes the main idea of constructing the algorithms for fitting TNPM. Specifically, let's consider a rearranged version $P(\mathbf{c}, \mathbf{z})$ of the matrix P , where the rows and columns are allocated based on community membership. For instance, nodes belonging to out (in) -community 1 occupy the first n_1 (m_1) rows (columns), nodes from out (in) -community 2 occupy the subsequent n_2 (m_2) rows (columns), and so on. We denote the (k, l) -th block of matrix $P(\mathbf{c}, \mathbf{z})$ as $P^{(k,l)}(\mathbf{c}, \mathbf{z})$. The sub-matrix $P^{(k,l)}(\mathbf{c}, \mathbf{z}) \in \mathbb{R}^{n_k \times m_l}$ corresponds to the nodes in the community pair $(\mathcal{N}_k, \mathcal{M}_l)$, respectively. Furthermore, we have $P_{ij}^{k,l} = \Lambda_{i_k l} \tilde{\Lambda}_{j_l k}$, where i_k represents the i -th element in \mathcal{N}_k and j_l represents the j -th element in \mathcal{M}_l . As a result, the matrices $P^{(k,l)}(\mathbf{c}, \mathbf{z})$ are rank-one matrices with unique singular vectors. In fact, we can express them as

$$P^{(k,l)}(\mathbf{c}, \mathbf{z}) = V^{(k,l)} \left[\tilde{V}^{(l,k)} \right]^T, \quad (2)$$

where $V^{(k,l)}$ and $\tilde{V}^{(l,k)}$ are vectors with elements $\tilde{V}_i^{(k,l)} = \Lambda_{i_k l}$, for $i \in [n_k]$ and $i_k \in \mathcal{N}_k$, and $\tilde{V}_j^{(l,k)} = \tilde{\Lambda}_{j_l k}$, for $j \in [m_l]$ and $j_l \in \mathcal{M}_l$. Therefore, we can rewrite $P(\mathbf{c}, \mathbf{z})$ as

$$P(\mathbf{c}, \mathbf{z}) = \begin{bmatrix} V^{(1,1)} \left(\tilde{V}^{(1,1)} \right)^T & V^{(1,2)} \left(\tilde{V}^{(2,1)} \right)^T & \dots & V^{(1,L)} \left(\tilde{V}^{(L,1)} \right)^T \\ V^{(2,1)} \left(\tilde{V}^{(1,2)} \right)^T & V^{(2,2)} \left(\tilde{V}^{(2,2)} \right)^T & \dots & V^{(2,L)} \left(\tilde{V}^{(L,2)} \right)^T \\ \vdots & \vdots & \dots & \vdots \\ V^{(K,1)} \left(\tilde{V}^{(1,K)} \right)^T & V^{(K,2)} \left(\tilde{V}^{(2,K)} \right)^T & \dots & V^{(K,L)} \left(\tilde{V}^{(L,K)} \right)^T \end{bmatrix}. \quad (3)$$

Rank-one structures have also been observed in undirected networks (Noroozi et al., 2021a,b). However, it remains a significant challenge to identify these structures without prior knowledge of the node memberships, especially when dealing with large K or/and L values. Direct application of previous methods can result in poor fitting performance and can also be time-consuming, as demonstrated in our empirical studies.

3 Methodology

In this section, we introduce the Delete-One-Method (DOM) and the Two-Stage Divided Cosine Algorithm (TSDC) for the purpose of model fitting and community detection under the TNPM.

3.1 The Delete-One-Method (DOM)

With the observation of the block rank-one structure shown in equation (3), we propose the objective function defined as follows:

$$Loss(\mathbf{c}, \mathbf{z}) = \sum_{k=1}^K \sum_{l=1}^L \left\| A^{(k,l)}(\mathbf{c}, \mathbf{z}) - V^{(k,l)} \left[\tilde{V}^{(l,k)} \right]^T \right\|_F^2, \quad (4)$$

where $A^{(k,l)}(\mathbf{c}, \mathbf{z})$ represents the (k, l) -th block of $A(\mathbf{c}, \mathbf{z})$, and $A(\mathbf{c}, \mathbf{z})$ is the rearranged matrix of A according to \mathbf{c} and \mathbf{z} .

To address the identifiability issue in the recovery of $V^{(k,l)}$ and $\tilde{V}^{(l,k)}$, we introduce $\Theta^{(k,l)}$ as the notation for $V^{(k,l)} \left[\tilde{V}^{(l,k)} \right]^T$ and focus on recovering the uniquely defined rank-one matrix $\Theta^{(k,l)}$. In addition, since the numbers of communities K and L are usually unknown, following the idea in Noroozi et al. (2021a,b), a penalty on K and L is introduced to safeguard against choosing too many communities. Consequently, our optimization problem can be formulated as follows:

$$\left(\hat{\Theta}, \hat{\mathbf{c}}, \hat{\mathbf{z}}, \hat{K}, \hat{L} \right) = \arg \min_{\mathbf{c}, \mathbf{z}, K, L} \left\{ \sum_{k=1}^K \sum_{l=1}^L \left\| A^{(k,l)}(\mathbf{c}, \mathbf{z}) - \Theta^{(k,l)} \right\|_F^2 + Pen(n, m, K, L) \right\} \quad (5)$$

$$\text{s.t. rank} \left(\Theta^{(k,l)} \right) = 1; \quad k \in [K]; \quad l \in [L],$$

where $\hat{\Theta}$ is the block matrix with blocks $\hat{\Theta}^{(k,l)}$, and $Pen(n, m, K, L)$ is the item of penalty and will be defined later.

If $\hat{\mathbf{c}}$, $\hat{\mathbf{z}}$, \hat{K} , and \hat{L} were known, the optimal solution to problem (5) would be obtained by the rank-one approximations $\hat{\Theta}^{(k,l)}$ of the sub-matrix $A^{(k,l)}(\hat{\mathbf{c}}, \hat{\mathbf{z}})$. These approximations can be expressed as

$$\hat{\Theta}^{k,l}(\hat{\mathbf{c}}, \hat{\mathbf{z}}) = \Pi_{\hat{u}, \hat{v}}(A^{(k,l)}(\hat{\mathbf{c}}, \hat{\mathbf{z}})) = \hat{\sigma}_1^{(k,l)} \hat{u}^{(k,l)}(\hat{\mathbf{c}}, \hat{\mathbf{z}}) (\hat{v}^{(k,l)}(\hat{\mathbf{c}}, \hat{\mathbf{z}}))^T \quad (6)$$

where $\hat{\sigma}_1^{(k,l)}$ represents the largest singular value of $A^{(k,l)}(\hat{\mathbf{c}}, \hat{\mathbf{z}})$, and $\hat{u}^{(k,l)}(\hat{\mathbf{c}}, \hat{\mathbf{z}})$ and $\hat{v}^{(k,l)}(\hat{\mathbf{c}}, \hat{\mathbf{z}})$ are the corresponding singular vectors. Here, the operation $\Pi(\cdot)$ denotes the rank-one projection. Plugging (6) into (5), the optimization problem (5) could be rewritten as

$$(\hat{\mathbf{c}}, \hat{\mathbf{z}}, \hat{K}, \hat{L}) = \arg \min_{\mathbf{c}, \mathbf{z}, K, L} \left\{ \sum_{k=1}^K \sum_{l=1}^L \left\| A_{(\mathcal{N}_k, \mathcal{M}_l)}^{(\mathbf{c}, \mathbf{z})} - \hat{\Theta}^{(k,l)} \right\|_F^2 + Pen(n, m, K, L) \right\}. \quad (7)$$

In order to obtain $(\hat{\mathbf{c}}, \hat{\mathbf{z}})$, one need to solve optimization problem (7) for every K and L , obtaining

$$(\hat{\mathbf{c}}_K, \hat{\mathbf{z}}_L) = \arg \min_{\substack{\mathbf{z} \in [L]^m \\ \mathbf{c} \in [K]^n}} \sum_{k=1}^K \sum_{l=1}^L \left\| A_{(\mathcal{N}_k, \mathcal{M}_l)}^{(\mathbf{c}, \mathbf{z})} - \prod_{\hat{u}, \hat{v}} (A_{(\mathcal{N}_k, \mathcal{M}_l)}^{(\mathbf{c}, \mathbf{z})}) \right\|_F^2, \quad (8)$$

and then find \hat{K} and \hat{L} as

$$(\hat{K}, \hat{L}) = \arg \min_{K, L} \left\{ \sum_{k=1}^K \sum_{l=1}^L \left\| A_{(\mathcal{N}_k, \mathcal{M}_l)}^{(\hat{\mathbf{c}}_K, \hat{\mathbf{z}}_L)} - \prod_{\hat{u}, \hat{v}} (A_{(\mathcal{N}_k, \mathcal{M}_l)}^{(\hat{\mathbf{c}}_K, \hat{\mathbf{z}}_L)}) \right\|_F^2 + Pen(n, m, K, L) \right\}. \quad (9)$$

The optimization problem (8) constitutes the most crucial part of the fitting algorithm, and its optimization is often NP-hard. Consequently, the development of efficient algorithms for approximating the optimization of (8) is of utmost significance. To address this challenge, we introduce an alternating update algorithm and integrate a Delete-One-Method (DOM) within the iteration process, resulting in a substantial reduction in computational complexity.

Specifically, at the t -th step, when $(\mathbf{c}^{(t)}, \mathbf{z}^{(t)})$ are given, we update \mathbf{c} and \mathbf{z} separately to obtain $\mathbf{c}^{(t+1)}$ and $\mathbf{z}^{(t+1)}$. To provide a detailed explanation, given $\mathbf{c}^{(t)}$ and $\mathbf{z}^{(t)}$, the sub-optimization task related to $\mathbf{c}^{(t+1)}$ can be expressed as

$$\mathbf{c}^{(t+1)} = \arg \min_{\mathbf{c} \in [K]^n} \sum_{k=1}^K \sum_{l=1}^L \left\| A_{(\mathcal{N}_k, \mathcal{M}_l)}^{(\mathbf{c}, \mathbf{z}^{(t)})} - \prod_{\hat{u}, \hat{v}} (A_{(\mathcal{N}_k, \mathcal{M}_l)}^{(\mathbf{c}, \mathbf{z}^{(t)})}) \right\|_F^2. \quad (10)$$

In particular, for each $i \in [n]$, we have:

$$\mathbf{c}_i^{(t+1)} = \arg \min_{\tilde{\mathbf{c}}_i^{(t)} \in [K]} \sum_{k=1}^K \sum_{l=1}^L \left\| A_{(\mathcal{N}_k, \mathcal{M}_l)}^{(\tilde{\mathbf{c}}_i^{(t)}, \mathbf{z}^{(t)})} - \prod_{\hat{u}, \hat{v}} (A_{(\mathcal{N}_k, \mathcal{M}_l)}^{(\tilde{\mathbf{c}}_i^{(t)}, \mathbf{z}^{(t)})}) \right\|_F^2, \quad (11)$$

where $\tilde{\mathbf{c}}_p^{(t)} = \mathbf{c}_p^{(t)}$ when $p \neq i$.

The minimization problem (11) is computationally expensive since it requires calculating the Frobenius norm error for each $K \times L$ block. To simplify this calculation, we propose subtracting

the value of the right side of (11) for A_{-i} , where A_{-i} refers to the adjacency matrix A with the i -th row deleted

$$\mathbf{c}_i^{(t+1)} = \arg \min_{\tilde{\mathbf{c}}_i^{(t)} \in [K]} \left\{ \sum_{k=1}^K \sum_{l=1}^L \left\| A_{(\mathcal{N}_k, \mathcal{M}_l)}^{(\tilde{\mathbf{c}}^{(t)}, \mathbf{z}^{(t)})} - \prod_{\hat{u}, \hat{v}} (A_{(\mathcal{N}_k, \mathcal{M}_l)}^{(\tilde{\mathbf{c}}^{(t)}, \mathbf{z}^{(t)})}) \right\|_F^2 - \sum_{k=1}^K \sum_{l=1}^L \left\| A_{(\mathcal{N}_k \setminus i, \mathcal{M}_l)}^{(\tilde{\mathbf{c}}^{(t)}, \mathbf{z}^{(t)})} - \prod_{\hat{u}, \hat{v}} (A_{(\mathcal{N}_k \setminus i, \mathcal{M}_l)}^{(\tilde{\mathbf{c}}^{(t)}, \mathbf{z}^{(t)})}) \right\|_F^2 \right\}.$$

Thus, we obtain the simplified expression as follows:

$$\mathbf{c}_i^{(t+1)} = \arg \min_{\tilde{\mathbf{c}}_i^{(t)} \in [K]} \left\{ \sum_{l=1}^L \left\| A_{(\mathcal{N}_{\tilde{\mathbf{c}}_i^{(t)}}, \mathcal{M}_l)}^{(\tilde{\mathbf{c}}^{(t)}, \mathbf{z}^{(t)})} - \prod_{\hat{u}, \hat{v}} (A_{(\mathcal{N}_{\tilde{\mathbf{c}}_i^{(t)}}, \mathcal{M}_l)}^{(\tilde{\mathbf{c}}^{(t)}, \mathbf{z}^{(t)})}) \right\|_F^2 - \sum_{l=1}^L \left\| A_{(\mathcal{N}_{\tilde{\mathbf{c}}_i^{(t)}} \setminus i, \mathcal{M}_l)}^{(\tilde{\mathbf{c}}^{(t)}, \mathbf{z}^{(t)})} - \prod_{\hat{u}, \hat{v}} (A_{(\mathcal{N}_{\tilde{\mathbf{c}}_i^{(t)}} \setminus i, \mathcal{M}_l)}^{(\tilde{\mathbf{c}}^{(t)}, \mathbf{z}^{(t)})}) \right\|_F^2 \right\}. \quad (12)$$

Similarly, the sub-optimization task related to $\mathbf{z}^{(t+1)}$ can be described as follows:

$$\mathbf{z}^{(t+1)} = \arg \min_{\mathbf{z} \in [L]^m} \left\{ \sum_{k=1}^K \sum_{l=1}^L \left\| A_{(\mathcal{N}_k, \mathcal{M}_l)}^{(\mathbf{c}^{(t+1)}, \mathbf{z})} - \prod_{\hat{u}, \hat{v}} (A_{(\mathcal{N}_k, \mathcal{M}_l)}^{(\mathbf{c}^{(t+1)}, \mathbf{z})}) \right\|_F^2 - \sum_{k=1}^K \sum_{l=1}^L \left\| A_{(\mathcal{N}_k, \mathcal{M}_{\tilde{\mathbf{z}}_j^{(t)} \setminus j})}^{(\mathbf{c}^{(t+1)}, \tilde{\mathbf{z}}^{(t)})} - \prod_{\hat{u}, \hat{v}} (A_{(\mathcal{N}_k, \mathcal{M}_{\tilde{\mathbf{z}}_j^{(t)} \setminus j})}^{(\mathbf{c}^{(t+1)}, \tilde{\mathbf{z}}^{(t)})}) \right\|_F^2 \right\}.$$

Consequently, for each $j \in [m]$, the sub-optimization task for $\mathbf{z}_j^{(t+1)}$ is defined as follows:

$$\mathbf{z}_j^{(t+1)} = \arg \min_{\tilde{\mathbf{z}}_j^{(t)} \in [L]} \left\{ \sum_{k=1}^K \left\| A_{(\mathcal{N}_k, \mathcal{M}_{\tilde{\mathbf{z}}_j^{(t)}})}^{(\mathbf{c}^{(t+1)}, \tilde{\mathbf{z}}^{(t)})} - \prod_{\hat{u}, \hat{v}} (A_{(\mathcal{N}_k, \mathcal{M}_{\tilde{\mathbf{z}}_j^{(t)}})}^{(\mathbf{c}^{(t+1)}, \tilde{\mathbf{z}}^{(t)})}) \right\|_F^2 - \sum_{k=1}^K \left\| A_{(\mathcal{N}_k, \mathcal{M}_{\tilde{\mathbf{z}}_j^{(t)} \setminus j})}^{(\mathbf{c}^{(t+1)}, \tilde{\mathbf{z}}^{(t)})} - \prod_{\hat{u}, \hat{v}} (A_{(\mathcal{N}_k, \mathcal{M}_{\tilde{\mathbf{z}}_j^{(t)} \setminus j})}^{(\mathbf{c}^{(t+1)}, \tilde{\mathbf{z}}^{(t)})}) \right\|_F^2 \right\}. \quad (13)$$

The overall process of the DOM algorithm can be summarized as in Algorithm 1.

In the initialization step of Algorithm 1, we employ a combination of SVD and K-means clustering to obtain $\mathbf{c}^{(0)}$ and $\mathbf{z}^{(0)}$. Given the adjacency matrix A , we initially apply SVD ($A \approx U\Sigma V^T$) to extract features from rows and columns. Here, $U \in \mathbb{R}^{n \times K}$ and $V \in \mathbb{R}^{m \times L}$ represent the row and column features, respectively. Subsequently, we employ K-means clustering on U and V to obtain the row cluster labels $\mathbf{c}^{(0)}$ and column cluster labels $\mathbf{z}^{(0)}$, respectively. Simulation studies have demonstrated that this initialization method yields more satisfactory results compared to other naive approaches.

Algorithm 1 Delete-One-Method Algorithm

Input: observed adjacency matrix A , ϵ , $iter_{\max}$

- 1: Initialization: $(\mathbf{c}^{(0)}, \mathbf{z}^{(0)})$, and set $t = 0$.
 - 2: **while** $t < iter_{\max}$ **do**
 - 3: **for** $i \leftarrow 1$ to n **do**
 - 4: $\mathbf{c}_i^{(t+1)}$ is calculated by (12) with $\{\mathbf{c}_1^{(t)}, \dots, \mathbf{c}_{i-1}^{(t)}\}$ replaced by $\{\mathbf{c}_1^{(t+1)}, \dots, \mathbf{c}_{i-1}^{(t+1)}\}$.
 - 5: **end for**
 - 6: **for** $j \leftarrow 1$ to m **do**
 - 7: $\mathbf{z}_j^{(t+1)}$ is calculated by (13) with $\{\mathbf{z}_1^{(t)}, \dots, \mathbf{z}_{j-1}^{(t)}\}$ replaced by $\{\mathbf{z}_1^{(t+1)}, \dots, \mathbf{z}_{j-1}^{(t+1)}\}$, and with $\mathbf{c}^{(t)}$ replaced by $\mathbf{c}^{(t+1)}$.
 - 8: **end for**
 - 9: **if** $\frac{|\mathbf{L}(\mathbf{c}^{(t+1)}, \mathbf{z}^{(t+1)}) - \mathbf{L}(\mathbf{c}^{(t)}, \mathbf{z}^{(t)})|}{\mathbf{L}(\mathbf{c}^{(t)}, \mathbf{z}^{(t)})} < \epsilon$ **then**
 - 10: break
 - 11: **end if**
 - 12: $t \leftarrow t + 1$
 - 13: **end while**
- Output:** return $\hat{\mathbf{c}} = \mathbf{c}^{(t)}$, $\hat{\mathbf{z}} = \mathbf{z}^{(t)}$.
-

3.2 Two-Stage Divided Cosine Algorithm (TSDC)

While the DOM algorithm successfully decreases computational complexity and can handle network data with thousands of nodes within an acceptable time range, it still has limitations when it comes to effectively deal with large-scale network data. Hence, to tackle this drawback, we propose a more computationally efficient algorithm called the Two-Stage Divided Cosine Algorithm (TSDC). The number of communities, denoted as K and L , is assumed to be known throughout this subsection.

Let's consider a block $P^{(k,l)}(\mathbf{c}, \mathbf{z})$, where out-node i and out-node j belong to the same community \mathcal{N}_k . In this case, corresponding to the i_k -th and j_k -th rows of $P^{(k,l)}(\mathbf{c}, \mathbf{z})$, as given by the equation (2), we have

$$P_{i_k}^{(k,l)}(\mathbf{c}, \mathbf{z}) = V_{i_k}^{(k,l)} \left(\tilde{V}^{(l,k)} \right)^T, P_{j_k}^{(k,l)}(\mathbf{c}, \mathbf{z}) = V_{j_k}^{(k,l)} \left(\tilde{V}^{(l,k)} \right)^T. \quad (14)$$

Thus, the cosine similarity between $P^{(k,l)}_{i_k}(\mathbf{c}, \mathbf{z})$ and $P^{(k,l)}_{j_k}(\mathbf{c}, \mathbf{z})$ is equal to 1. However, when out-node i and out-node j do not belong to the same community, the cosine similarity between $P^{(k,l)}_{i_k}(\mathbf{c}, \mathbf{z})$ and $P^{(k,l)}_{j_k}(\mathbf{c}, \mathbf{z})$ is strictly less than 1 under the assumption of pairwise linear independence, i.e. $\tilde{V}^{(l,k)}$ and $\tilde{V}^{(l,k')}$ are linearly independent for any $k \neq k'$.

In view of this, we propose a similarity measure called Block Cosine Similarity to combine cosine similarities throughout all the column communities. Let A_i and A_j denote the i -th and j -th rows of A , respectively. Given the column community label \mathbf{z} , the Block Cosine Similarity between A_i and A_j is defined as

$$BlockCos(A_i, A_j) = \sum_{l=1}^L \cos(A_{i\mathcal{M}_l}, A_{j\mathcal{M}_l}).$$

Similarly, for any two in-nodes i and j , given the row community label \mathbf{c} , the Block Cosin Similarity between $A_{\cdot i}$ and $A_{\cdot j}$ is defined as:

$$\text{BlockCos}(A_{\cdot i}, A_{\cdot j}) = \sum_{l=1}^K \cos(A_{\mathcal{N}_k i}, A_{\mathcal{N}_k j}).$$

Basing on the Block Cosin Similarity, we propose a two-stage algorithm to facilitate the community detection for both rows and columns. The first stage aims to detect the row assignment \mathbf{c} given \mathbf{z} , and the corresponding objective function is defined as

$$\mathbf{L}(\mathbf{c}|\mathbf{z}) = \sum_{i=1}^n \text{BlockCos}(A_{i\cdot}, \boldsymbol{\mu}_{\mathbf{c}_i \cdot})/L.$$

Here, $\boldsymbol{\mu} \in \mathbb{R}^{K \times m}$ represents the community centers for rows, and the similarity function used is the *BlockCos*. Similarly, in the second stage, we update \mathbf{z} given \mathbf{c} , and the objective function is defined as

$$\tilde{\mathbf{L}}(\mathbf{z}|\mathbf{c}) = \sum_{j=1}^m \text{BlockCos}(A_{\cdot j}, \tilde{\boldsymbol{\mu}}_{\cdot \mathbf{z}_j})/K,$$

where $\tilde{\boldsymbol{\mu}} \in \mathbb{R}^{n \times L}$ represents the column community centers.

The proposed objective function is minimized by alternatively updating (\mathbf{c}, \mathbf{z}) and $(\boldsymbol{\mu}, \tilde{\boldsymbol{\mu}})$. Specifically, given $(\mathbf{c}^{(t)}, \mathbf{z}^{(t)})$ at the t -th step, we first obtain $(\boldsymbol{\mu}^{(t)}, \tilde{\boldsymbol{\mu}}^{(t)})$ through the suboptimization task

$$\begin{aligned} \boldsymbol{\mu}^{(t)} &= \max_{\boldsymbol{\mu}} \mathbf{L}(\mathbf{c}^{(t)}|\mathbf{z}^{(t)}) = \max_{\boldsymbol{\mu}} \sum_{i=1}^n \text{BlockCos}(A_{i\cdot}, \boldsymbol{\mu}_{\mathbf{c}_i \cdot})/L, \\ \tilde{\boldsymbol{\mu}}^{(t)} &= \max_{\tilde{\boldsymbol{\mu}}} \tilde{\mathbf{L}}(\mathbf{z}^{(t)}|\mathbf{c}^{(t)}) = \max_{\tilde{\boldsymbol{\mu}}} \sum_{j=1}^m \text{BlockCos}(A_{\cdot j}, \tilde{\boldsymbol{\mu}}_{\cdot \mathbf{z}_j})/K. \end{aligned}$$

Given a block $P^{(k,l)}(\mathbf{c}, \mathbf{z})$, its row cluster center, $\mu_{k, \tilde{\mathcal{N}}_l} \in \mathbb{R}^{\tilde{n}_l}$, and column cluster center, $\tilde{\mu}_{\mathcal{N}_k, l} \in \mathbb{R}^{n_k}$, can be derived as

$$\mu_{k, \tilde{\mathcal{N}}_l} = \frac{\mu'_{k, \tilde{\mathcal{N}}_l}}{\|\mu'_{k, \tilde{\mathcal{N}}_l}\|_1} \times \tilde{n}_l, \quad \text{where} \quad \mu'_{k, \tilde{\mathcal{N}}_l} = \frac{\sum_{i=1}^{n_k} P_{i\cdot}^{(k,l)}(\mathbf{c}, \mathbf{z})}{\|P_{i\cdot}^{(k,l)}(\mathbf{c}, \mathbf{z})\|_2}, \quad (15)$$

$$\tilde{\mu}_{\mathcal{N}_k, l} = \frac{\tilde{\mu}'_{\mathcal{N}_k, l}}{\|\tilde{\mu}'_{\mathcal{N}_k, l}\|_1} \times n_k, \quad \text{where} \quad \tilde{\mu}'_{\mathcal{N}_k, l} = \frac{\sum_{j=1}^{\tilde{n}_l} P_{\cdot j}^{(k,l)}(\mathbf{c}, \mathbf{z})}{\|P_{\cdot j}^{(k,l)}(\mathbf{c}, \mathbf{z})\|_2}. \quad (16)$$

Combining the cluster centers for each block, we obtain

$$\boldsymbol{\mu} = \begin{pmatrix} \mu_{11} & \mu_{12} & \cdots & \mu_{1m} \\ \mu_{21} & \mu_{22} & \cdots & \mu_{2m} \\ \vdots & \vdots & & \vdots \\ \mu_{K1} & \mu_{K2} & \cdots & \mu_{Km} \end{pmatrix} \in \mathbb{R}^{K \times m}, \quad \tilde{\boldsymbol{\mu}} = \begin{pmatrix} \tilde{\mu}_{11} & \tilde{\mu}_{12} & \cdots & \tilde{\mu}_{1L} \\ \tilde{\mu}_{21} & \tilde{\mu}_{22} & \cdots & \tilde{\mu}_{2L} \\ \vdots & \vdots & & \vdots \\ \tilde{\mu}_{n1} & \tilde{\mu}_{n2} & \cdots & \tilde{\mu}_{nL} \end{pmatrix} \in \mathbb{R}^{n \times L}.$$

We update \mathbf{c} and \mathbf{z} separately to obtain $\mathbf{c}^{(t+1)}$ and $\mathbf{z}^{(t+1)}$. Given $\mathbf{c}^{(t)}$, $\mathbf{z}^{(t)}$, $\boldsymbol{\mu}^{(t)}$, $\tilde{\boldsymbol{\mu}}^{(t)}$, the optimization task related to $\mathbf{c}^{(t+1)}$ becomes

$$\max_{\mathbf{c}} \mathbf{L}(\mathbf{c}|\mathbf{z}^{(t)}) = \max_{\mathbf{c}} \sum_{i=1}^n \text{BlockCos}(A_{i\cdot}, \boldsymbol{\mu}_{\mathbf{c}_i}^{(t)})/L.$$

Specially, for each $i \in [n]$,

$$\mathbf{c}_i^{(t+1)} = \arg \max_{1 \leq c_i \leq K} \text{BlockCos}(A_{i\cdot}, \boldsymbol{\mu}_{\mathbf{c}_i}^{(t)})/L.$$

Similarly, the sub-optimization task related to $\mathbf{z}^{(t+1)}$ is

$$\max_{\mathbf{z}} \tilde{\mathbf{L}}(\mathbf{z}|\mathbf{c}^{(t+1)}) = \max_{\mathbf{z}} \sum_{j=1}^m \text{BlockCos}(A_{\cdot j}, \tilde{\boldsymbol{\mu}}_{\mathbf{z}_j}^{(t)})/K.$$

Thus, for each $j \in [m]$,

$$\mathbf{z}_j^{(t+1)} = \arg \max_{1 \leq z_j \leq L} \text{BlockCos}(A_{\cdot j}, \tilde{\boldsymbol{\mu}}_{\mathbf{z}_j}^{(t)})/K.$$

Next, given $\mathbf{c}^{(t+1)}$ and $\mathbf{z}^{(t+1)}$, we update $\boldsymbol{\mu}$ and $\tilde{\boldsymbol{\mu}}$ using equations (15) and (16), respectively. The whole algorithm can be summarized as shown in Algorithm 2. The initialization of $(\mathbf{c}^{(0)}, \mathbf{z}^{(0)})$ follows the same procedure as in the DOM method.

Algorithm 2 Two-stage Divided Cosine Algorithm

Input: observed adjacency matrix A , ϵ , $iter_{\max}$

- 1: Initialization: $(\mathbf{c}^{(0)}, \mathbf{z}^{(0)})$, and set $t = 0$.
- 2: **while** $t < iter_{\max}$ **do**
- 3: $\boldsymbol{\mu}^{(t)}$ and $\tilde{\boldsymbol{\mu}}^{(t)}$ are calculated according to (15) and (16), respectively.
- 4: $\mathbf{c}_i^{(t+1)} = \arg \max_{1 \leq c_i \leq K} \text{BlockCos}(A_{i\cdot}, \boldsymbol{\mu}_{\mathbf{c}_i}^{(t)})$, $1 \leq i \leq n$.
- 5: $\mathbf{z}_j^{(t+1)} = \arg \max_{1 \leq z_j \leq L} \text{BlockCos}(A_{\cdot j}, \tilde{\boldsymbol{\mu}}_{\mathbf{z}_j}^{(t)})$, $1 \leq j \leq m$.
- 6: **if** $\frac{|\mathbf{L}(\mathbf{c}^{(t+1)}, \mathbf{z}^{(t+1)}) - \mathbf{L}(\mathbf{c}^{(t)}, \mathbf{z}^{(t)})|}{\mathbf{L}(\mathbf{c}^{(t)}, \mathbf{z}^{(t)})} < \epsilon$ **then**
- 7: **break**
- 8: **end if**
- 9: $t \leftarrow t + 1$
- 10: **end while**

Output: return $\hat{\mathbf{c}} = \mathbf{c}^{(t)}$, $\hat{\mathbf{z}} = \mathbf{z}^{(t)}$.

4 Consistency Results

In this section, we demonstrate the identifiability of the community structure under the TNPM model and establish the consistency of the DOM algorithm. This includes the consistency of estimating the

connection probability matrix and the consistency of community detection. For generality, throughout this section, we assume that each entry A_{ij} of the adjacency matrix A follows a sub-Gaussian distribution with variance proxy σ_{ij}^2 when \mathbf{c} and \mathbf{z} are given. Specifically, given \mathbf{c} and \mathbf{z} , it has

$$A_{ij} - \mathbb{E}(A_{i,j}|\mathbf{c}, \mathbf{z}) \sim \text{subG}(\sigma_{ij}^2), \quad \text{for any } i \in [n], j \in [m], \quad (17)$$

where σ_{ij}^2 satisfies that

$$\mathbb{E}[\exp(t\{A_{ij} - \mathbb{E}(A_{i,j}|\mathbf{c}, \mathbf{z})\})] \leq \exp\left(\frac{\sigma_{ij}^2 t^2}{2}\right), \quad \forall t \in \mathbb{R}.$$

Note that $\text{subG}(\sigma^2)$ denotes a class of distributions rather than a distribution. Therefore, the notation is slightly abused when writing some random variable $X \sim \text{subG}(\sigma^2)$. All the proofs and technical details are presented in the Appendix A and B.

4.1 Identifiability of Community Structure

We first demonstrate the identifiability of community structures under the TNPM model, assuming numbers of communities, K and L , are known. According to the model setting, the parameters Λ and $\tilde{\Lambda}$ have the following structure

$$\Lambda = \begin{pmatrix} \Lambda_{11} & \Lambda_{12} & \cdots & \Lambda_{1L} \\ \Lambda_{21} & \Lambda_{22} & \cdots & \Lambda_{2L} \\ \vdots & \vdots & & \vdots \\ \Lambda_{K1} & \Lambda_{K2} & \cdots & \Lambda_{KL} \end{pmatrix}, \quad \tilde{\Lambda} = \begin{pmatrix} \tilde{\Lambda}_{11} & \tilde{\Lambda}_{12} & \cdots & \tilde{\Lambda}_{1K} \\ \tilde{\Lambda}_{21} & \tilde{\Lambda}_{22} & \cdots & \tilde{\Lambda}_{2K} \\ \vdots & \vdots & & \vdots \\ \tilde{\Lambda}_{L1} & \tilde{\Lambda}_{L2} & \cdots & \tilde{\Lambda}_{LK} \end{pmatrix}.$$

To analyze the identifiability of the community structure under TNPM, we make the following assumptions:

Assumption A1: All of the elements in Λ and $\tilde{\Lambda}$ are positive.

Assumption A2: The points in the same community are in *general position*, which implies that any subset of L rows of the matrix $\Lambda_k = [\Lambda_{k1}, \Lambda_{k2}, \dots, \Lambda_{kL}]$ are linearly independent for any $k \in [K]$, and any subset of K rows of the matrix $\tilde{\Lambda}_l = [\tilde{\Lambda}_{l1}, \tilde{\Lambda}_{l2}, \dots, \tilde{\Lambda}_{lK}]$ are linearly independent for any $l \in [L]$.

Assumption A3: $n \geq K^2L$ or $m \geq L^2K$.

Remark 1 : Assumptions A1, and A2 impose conditions and restrictions on the parameters Λ and $\tilde{\Lambda}$, and have also been employed in prior works such as Sengupta and Chen (2018) and Noroozi et al. (2021b). Assumption A3 introduces the lower bound of the network scale (n, m) according to the number of communities, K and L . Given that real-world networks often consist of a large number of nodes, while the number of communities is typically small, this assumption is naturally satisfied.

Theorem 1 *Under the TNPM, assuming that Assumptions A1~A3 hold, we consider the following optimization problem*

$$(\hat{\mathbf{c}}, \hat{\mathbf{z}}) = \arg \min_{\mathbf{c} \in [K]^n, \mathbf{z} \in [L]^m} \text{Loss}(\mathbf{c}, \mathbf{z}),$$

with

$$\begin{aligned} \text{Loss}(\mathbf{c}, \mathbf{z}) &= \sum_{k=1}^K \sum_{l=1}^L \left\| P^{(k,l)}((\mathbf{c}, \mathbf{z}) - \Pi_1 \{P^{(k,l)}(\mathbf{c}, \mathbf{z})\}) \right\|_F^2, \\ &= \min_{\substack{\lambda_{kl}, k \in [K], l \in [L] \\ \mu \in R^{K \times n}, \tilde{\mu} \in R^{m \times L}}} \sum_{k=1}^K \sum_{l=1}^L \left\| P^{(k,l)}(\mathbf{c}, \mathbf{z}) - \lambda_{kl} \tilde{\mu}_{[c=k], l} \mu_{k, [z=l]} \right\|_2^2, \end{aligned}$$

where \mathbf{c}, \mathbf{z} represent the clustering vectors. Then, we have $\hat{\mathbf{c}} \equiv \mathbf{c}^*$ and $\hat{\mathbf{z}} \equiv \mathbf{z}^*$, where \mathbf{c}^* and \mathbf{z}^* are the ground truth community structures, and \equiv indicates that the two community label assignments on both sides coincide up to a permutation π on $\{1, 2, \dots, K\}$ or $\{1, 2, \dots, L\}$.

Remark 2 : Theorem 1 provides the conditions for identifiability and demonstrates that under these assumptions, the ground truth community structures \mathbf{c}^* and \mathbf{z}^* can be uniquely determined by the mean structure of the adjacency matrix $P = \mathbb{E}(A)$.

4.2 Consistency of Estimated Connection Probability Matrix

In this subsection, we evaluate the error associated with the estimated connectivity probability matrix, which is obtained by using the DOM algorithm. The penalty term involved in the DOM algorithm is carefully chosen to exceed the random errors (See inequality (A.21) in the Appendix A). Specifically, we introduce the penalty as

$$\text{Pen}(n, m, K, L) = 2\tilde{\sigma}_{max}^2 \{(1 + 1/\alpha_2)F_1(n, m, K, L) + (1/\alpha_1)F_2(n, m, K, L)\}, \quad (18)$$

where $\tilde{\sigma}_{max}^2$ is an absolute constant, specified in advance, and not smaller than $\sigma_{max}^2 \triangleq \max_{i \in [n], j \in [m]} \sigma_{ij}^2$. Since σ_{max}^2 is unknown in real applications, we need to choose a sufficiently large but reasonable $\tilde{\sigma}_{max}^2$. $F_1(n, m, K, L)$ and $F_2(n, m, K, L)$ are defined as

$$\begin{aligned} F_1(n, m, K, L) &= C \{nL + mK + KL \log(2KL) + KL(n \log K + \log n + m \log L + \log m)\}, \\ F_2(n, m, K, L) &= n \log K + \log n + m \log L + \log m. \end{aligned}$$

Note that the constants $\{\alpha_1, \alpha_2, C\}$ involved above are all positive values that can be calculated, given in the proof of the following Theorem 2.

Theorem 2 Under the TNPM with $\sigma_{max}^2 \triangleq \max_{i \in [n], j \in [m]} \sigma_{ij}^2$, let $(\hat{K}, \hat{L}, \hat{\mathbf{c}}, \hat{\mathbf{z}})$ defined as

$$\begin{aligned} (\hat{K}, \hat{L}, \hat{\mathbf{c}}, \hat{\mathbf{z}}) &= \arg \min_{(K, L, \mathbf{c}, \mathbf{z})} \left\{ \sum_{k=1}^K \sum_{l=1}^L \left\| A^{(k,l)}(\mathbf{c}, \mathbf{z}) - \Pi_1 \{A^{(k,l)}(\mathbf{c}, \mathbf{z})\} \right\|_F^2 \right. \\ &\quad \left. + \text{Pen}(n, m, K, L) \right\}, \quad (19) \end{aligned}$$

then $\left\| \widehat{P} - P_* \right\|_F^2 = \sum_{k=1}^{\widehat{K}} \sum_{l=1}^{\widehat{L}} \left\| \Pi_1 \{A^{(k,l)}(\widehat{c}, \widehat{z})\} - P_*^{(k,l)}(\widehat{c}, \widehat{z}) \right\|_F^2$ satisfies the following inequalities

for any $t \geq 0$ and some positive constants $H_1 = \frac{1}{1-\alpha_1-4\alpha_2}$, $H_2 = \frac{2C+2/\alpha_1+2C/\alpha_2}{1-\alpha_1-4\alpha_2}$:

$$\mathbb{P} \left\{ \frac{1}{nm} \left\| \widehat{P} - P_* \right\|_F^2 \leq \frac{H_1}{nm} Pen(n, m, K_*, L_*) + \frac{H_2 \sigma_{max}^2}{nm} t \right\} \geq 1 - 3e^{-t}, \quad (20)$$

$$\frac{1}{nm} \mathbb{E} \left\| \widehat{P} - P_* \right\|_F^2 \leq \frac{H_1}{nm} Pen(n, m, K_*, L_*) + \frac{3H_2 \sigma_{max}^2}{nm}. \quad (21)$$

Remark 3 : Theorem 2 guarantees the consistency of the estimated connectivity probability matrix obtained by using the DOM algorithm under the TNPM model. The estimation remains consistent when $\frac{KL \log(KL)}{n \wedge m} \rightarrow 0$. In fact, according to the equation (18) and inequality (21), $Pen(n, m, K, L)$ converges to 0 when $\frac{KL \log(KL)}{n \wedge m} \rightarrow 0$.

Remark 4 : Theorem 2 significantly differs from the theoretical result in Noroozi et al. (2021b). First, we greatly extend the applicable types of networks, including binary networks, discrete-valued networks, continuous-valued networks, and even with mixture link distributions. Second, we use a new strategy to directly upper bound the operator norm of random matrices with sub-Gaussian entries. Following Noroozi et al. (2021b) will lead to the concentration inequality for the Lipschitz function of independent sub-Gaussian random variables, while it remains a highly challenging research topic in the academic community.

4.3 Consistency of Community Detection

In this subsection, we evaluate the error associated with the estimated community structure obtained by using the DOM algorithm. For the convenience of theoretical analysis, we assume that the true number of communities $K = K^*$ and $L = L^*$ is known, like Noroozi et al. (2021a,b).

Let $C_* \in \mathcal{M}_{n,K}$ denote the ground truth out-community matrix, $Z_* \in \mathcal{M}_{m,L}$ denote the ground truth in-community matrix. Let C and Z represent other out-community and in-community matrices, respectively. We define the proportion of misclassified nodes by C and Z as follows:

$$\begin{aligned} \text{Err}(C, C_*) &= (2n)^{-1} \min_{\mathcal{P}_K \in \mathbb{P}_K} \|C \mathcal{P}_K - C_*\|_1 = (2n)^{-1} \min_{\mathcal{P}_K \in \mathbb{P}_K} \|C \mathcal{P}_K - C_*\|_F^2, \\ \text{Err}(Z, Z_*) &= (2m)^{-1} \min_{\mathcal{P}_L \in \mathbb{P}_L} \|Z \mathcal{P}_L - Z_*\|_1 = (2m)^{-1} \min_{\mathcal{P}_L \in \mathbb{P}_L} \|Z \mathcal{P}_L - Z_*\|_F^2, \end{aligned}$$

where \mathbb{P}_K is the set of permutation matrices $\mathcal{P}_K : \{1, 2, \dots, K\} \rightarrow \{1, 2, \dots, K\}$, and \mathbb{P}_L is the set of permutation matrices $\mathcal{P}_L : \{1, 2, \dots, L\} \rightarrow \{1, 2, \dots, L\}$. Additionally, we define

$$\Upsilon(C_*, Z_*, \rho_{n,m}) = \{(C, Z) \in \mathcal{M}_{n,K} \times \mathcal{M}_{m,L} : \max\{\text{Err}(C, C_*), \text{Err}(Z, Z_*)\} \geq \rho_{n,m}\}$$

as the set of community matrices with the proportion of misclassified nodes being at least $\rho_{n,m} \in (0, 1)$.

Theorem 3 Under the TNPM with $\sigma_{max}^2 \triangleq \max_{i \in [n], j \in [m]} \sigma_{ij}^2$, assuming that Assumptions A1 ~ A3 hold, let $(\widehat{C}, \widehat{Z}) \equiv (\widehat{C}_K, \widehat{Z}_L)$ be the community matrices corresponding to (19). If there exist $\alpha \in (0, 1/2)$ and $\rho_{n,m} \in (0, 1)$ such that the following inequality holds

$$\begin{aligned} & \left\| P_* \right\|_F^2 - (1 + \alpha) \max_{(C, Z) \in \Upsilon(C_*, Z_*, \rho_{n,m})} \sum_{k=1}^K \sum_{l=1}^L \|P_*^{(k,l)}(C, Z)\|_{op}^2 \\ & \geq \sigma_{max}^2 [H_1 \{nL + mK + KL \log(2KL) + KL(m + n)\} + H_2 KL(n \log K + m \log L)], \end{aligned} \quad (22)$$

where α , H_1 and H_2 are absolute positive constants with their definitions provided the proof of this theorem. Then, with probability at least $1 - 2e^{-(n+m)}$, the proportion of nodes misclassified by (\hat{C}, \hat{Z}) is at most $\rho_{n,m}$, i.e.,

$$\max \{ \text{Err}(C, C_*), \text{Err}(Z, Z_*) \} \leq \rho_{n,m}. \quad (23)$$

Remark 5 : The condition (23) means that if the community matrices (C, Z) fall within the set where the proportion of misclassified nodes is at least $\rho_{n,m}$, there will exist a lower bound on the sum of the differences between the Frobenius and operator norms of the blocks $\{P_*^{(k,l)}(C, Z)\}$. In fact, if the clustering is incorrect, the ranks of the blocks would increase which would result in a discrepancy between their operator and Frobenius norms.

Remark 6 : Theorem 3 provides an upper bound on the misclassification rate, going beyond the conventional statement that it tends to zero as the network size increases, as it is routinely done in papers that rely on modularity maximization for clustering assignments (see, e.g. Bickel and Chen (2009); Zhao et al. (2012); Sengupta and Chen (2018)). Similar conclusion for undirected networks is obtained in Noroozi et al. (2021b). To the best of our knowledge, this is the cutting-edge result available so far.

5 Simulation Studies

In this section, we evaluate the performance of our proposed methods using synthetic networks, concentrating on two main aspects: the accuracy of community detection and computational efficiency. The code is publicly available at Github (<https://github.com/Wangya1996/Two-way-Node-Popularity-Model>).

5.1 Accuracy of Community Detection

The adjacency matrix A is generated element-wisely using Normal, Bernoulli, and Poisson distributions, guided by a probability matrix P defined by the TNPM model. Additionally, a mixture of Normal and Bernoulli distributions is examined to validate our theoretical findings in sub-Gaussian contexts. We only show the Normal and Normal-Bernoulli mixture generation cases here, and the rest are in the Appendix C..

The pair of community number (K, L) are set to be (3,4). We first assume that K and L are known, and will later consider the estimation of K and L . The elements of block matrices Λ and $\tilde{\Lambda}$ are drawn independently from $U[0, 1]$. The ground truth out-community assignments $\mathbf{c} \in [K]^n$ and in-community assignments $\mathbf{z} \in [L]^m$ are generated from a multinomial distribution, such that $P(\mathbf{c}_i = k) = 1/K$ and $P(\mathbf{z}_j = l) = 1/L$, where $k \in [K]$ and $l \in [L]$. Furthermore, for evaluating our methods in sparse data situations, we introduce a sparsity parameter η as the proportion of nonzero entries in matrix Λ and $\tilde{\Lambda}$. To induce sparsity, we set the $\lfloor nL\eta \rfloor$ ($\lfloor mK\eta \rfloor$) smallest non-diagonal entries of Λ ($\tilde{\Lambda}$) to zero.

We evaluate the performance of our proposed methods in comparison to current state-of-the-art approaches: OMPSC: A sparse subspace clustering method introduced by Noroozi et al. (2021b); COSSC and INSC: Both methods employ spectral clustering techniques, with COSSC leveraging a cosine similarity-based matrix and INSC utilizing an inner product similarity matrix; SVDK: This approach implements the K-means algorithm on the singular matrices derived from the network’s adjacency matrix.

Note that OMPSC, COSSC, and INSC are fundamentally developed for symmetric networks. To facilitate their application in analyzing directed or bipartite networks, we separately apply these methods to both the network’s adjacency matrix and its transpose. All the simulation results are based on 100 independent replications.

For community detection, we compare the performance of the DOM and TSDC algorithms against other techniques using three metrics: the clustering error in Wang (2010) and Zhang et al. (2021), the normalized mutual information (NMI) in Lancichinetti et al. (2009) and Zhou and Amini (2020), and the proportion of misclustered nodes in Noroozi et al. (2021a,b). Details on these metrics are accessible in Appendix C.1. This section primarily highlights the results using the NMI metric, while additional metrics results are provided in Appendix C.1.

We explore three distinct scenarios and the simulation settings are outlined as follows:

- *Normal case*: The node counts (n, m) are set as $(600, 600)$. The adjacency matrix $A = (A_{ij})$ is generated with entries $A_{ij} \sim \mathcal{N}(P_{ij}, \sigma^2)$, and σ is varied from 0 to 0.6 with the increment of 0.1.
- *Normal-Bernoulli Mixture case*: The values of n and m range from 360 to 1320, increasing in increments of 240. The lower half of the adjacency matrix A is filled with Bernoulli variables $A_{ij} \sim \text{Ber}(P_{ij})$ for $i \in [n]$ and $j = 1, \dots, i - 1$. When $j > i$, entries follow a normal distribution $A_{ij} \sim \mathcal{N}(P_{ij}, \sigma^2)$, with σ fixed at 0.1.
- *Sparse case*: The values of n and m range from 200 to 1000, increasing in increments of 100, while the sparsity parameter η is chosen from $\{0.3, 0.5, 0.7\}$. The adjacency matrix A is generated with Bernoulli variables $A_{ij} \sim \text{Ber}(P_{ij})$.

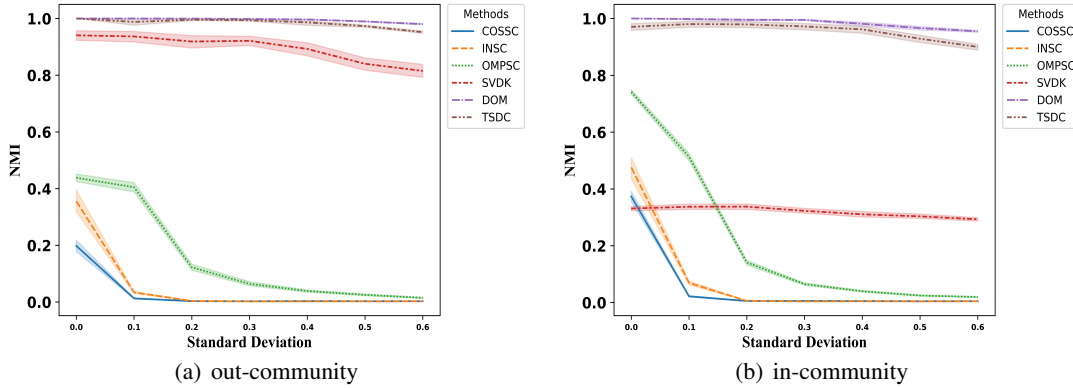


Figure 2: The NMI for Normal data generation case with $(n, m) = (600, 600)$. The left panel depicts out-community clustering, while the right panel shows in-community clustering.

Figures 2 and 3 clearly demonstrate that the DOM and TSDC algorithms exceed the performance of other methods. Appendix C.1 corroborates these findings, presenting consistent outcomes via the metrics of Misclassification Score (MIS) and Clustering Error.

From Figure 4, an increase in sparsity (η increases) correlates with a decrease in NMI. Additionally, the DOM method outperforms the TSDC method, especially in scenarios involving smaller

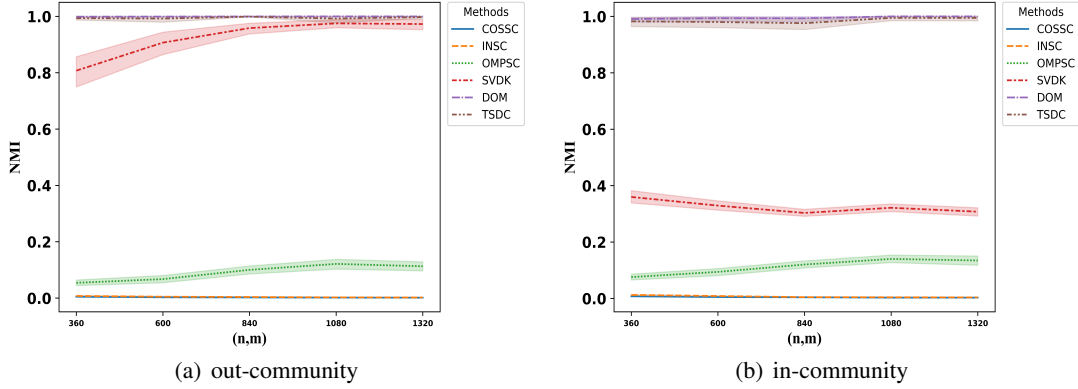


Figure 3: The NMI for Normal-Bernoulli mixture data generation case. The left panel depicts out-community clustering, while the right panel shows in-community clustering.

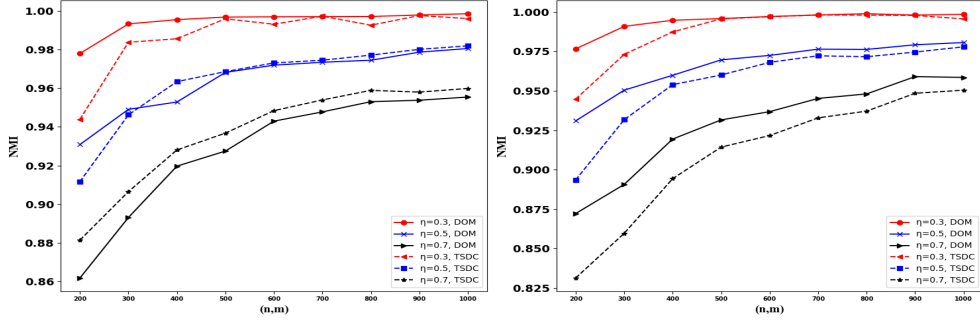


Figure 4: The NMI for sparsity data generation case. The left panel depicts out-community clustering, while the right panel shows in-community clustering.

networks and lower levels of sparsity. However, as the network size grows, the distinction between the DOM and TSDC results narrows.

5.2 Computational Efficiency

In this section, We assess the computational efficiency of each method by measuring the running time (in seconds). All methods are implemented in Matlab and run on a single processor of an Intel(R) Core(TM) i9-12900K CPU 3.20 GHz PC.

We set the values of n and m range from 360 to 1320, increasing in increments of 240 and generate the adjacency matrix $A = (A_{ij})$ where $A_{ij} \sim \mathcal{N}(P_{ij}, \sigma^2)$ with σ is chosen from $\{0.1, 0.5\}$. The computational efficiency of each algorithm, based on the average runtime from 100 simulations, is summarized in Table 1. The results reveal that the TSDC algorithm significantly outperforms the DOM algorithm in terms of processing speed, and a finding echoed in Appendix C.1 for matrices generated from Bernoulli and Poisson distributions. As noise levels rise, so does the computation time. This suggests the DOM algorithm as a viable option for smaller networks or non-urgent processing, whereas TSDC stands out for larger networks or scenarios requiring quick processing.

σ	(n, m)	DOM	TSDC	OMPSC	COSSC	INSC	SVDK
0.1	(360,360)	45.44	0.07	0.90	0.11	0.19	0.03
	(600,600)	173.12	0.13	2.56	0.25	0.64	0.06
	(840,840)	421.12	0.21	5.84	0.47	1.45	0.10
	(1080,1080)	892.90	0.27	11.08	0.78	2.95	0.15
	(1320,1320)	1482.88	0.57	14.34	0.97	5.41	0.19
0.5	(360,360)	66.45	0.27	0.93	0.11	0.19	0.03
	(600,600)	249.91	0.26	2.67	0.26	0.64	0.06
	(840,840)	592.11	0.37	5.96	0.49	1.46	0.10
	(1080,1080)	1219.89	0.49	11.30	0.80	2.94	0.15
	(1320,1320)	1657.89	0.59	14.87	0.98	5.38	0.19

Table 1: Running time (in seconds) for scenarios with n and m varying from 360 to 1320 in increments of 240, under the Normal data generation case for $\sigma=0.1,0.5$.

5.3 Unknown number of clusters

In our previous simulations, the true number of clusters K and L are given. If not, they can be estimated as solving the optimization problem (7), which can be equivalently rewritten as

$$\left(\hat{K}, \hat{L}\right) = \arg \min_{K, L} \left\{ \left\| A - \hat{P} \right\|_F^2 + Pen(n, m, K, L) \right\}. \quad (24)$$

We study the selection of unknown K (L) using an empirical version of this penalty

$$Pen(n, m, K, L) = \rho(A) \{ nL \sqrt{\ln n \ln L^3} + mK \sqrt{\ln m \ln K^3} \} \quad (25)$$

Table 3, 4 in Appendix C.3 present the relative frequencies of the estimator (\hat{K}, \hat{L}) of (K, L) chosen from $\{(3, 3), (4, 3), (4, 4)\}$, $n = 360$ and $\sigma=0.1,0.3,0.5$. It corroborates that, in the majority of cases, $(\hat{K}, \hat{L}) = (K, L)$, demonstrating that the estimation method reliably identifies the number of clusters with high probability.

6 Real Data Applications

In this section, we apply the DOM and TSDC algorithms to analyze two real datasets: the Worldwide Food Trading Networks data set and the MovieLens 100K data set.

6.1 Worldwide Food Trading Networks

The Worldwide Food Trading Networks is collected by De Domenico et al. (2015) and is available at <http://www.fao.org>. Our analysis focuses on trading data in 2010, specifically on two product categories: cereals and cigarettes. We exclude countries with negligible trading volume

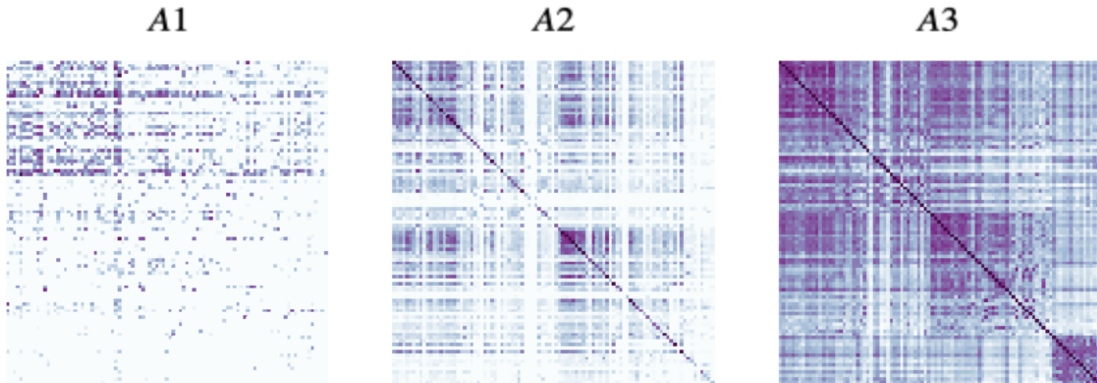


Figure 5: $A1$ displays the original cereal trading network, while $A2$ and $A3$ represent the block cosine similarity matrix for the rows and columns, respectively, with nodes ordering based on detected clustering labels.

(the first quartile), remaining 93 countries. Following the logarithmic transformation, we derive two directed 93×93 networks.

The DOM and TSDC algorithms are implemented on two networks, with parameters K and L set as 2 and 3, respectively. The results obtained from the DOM algorithm are presented here, and TSDC's are in Appendix D.1.

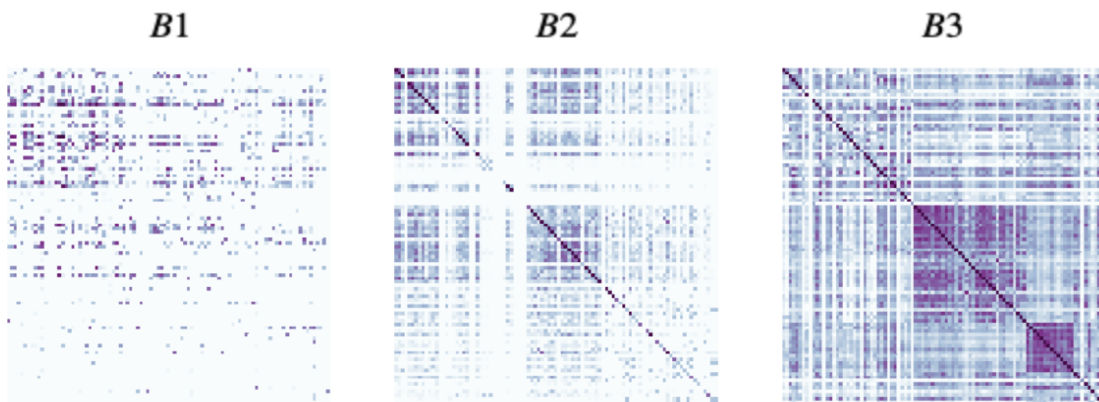


Figure 6: $B1$ displays the original trading cigarette network, with Figures $B2$ and $B3$ showcasing the reordered row and column block cosine similarity matrix.

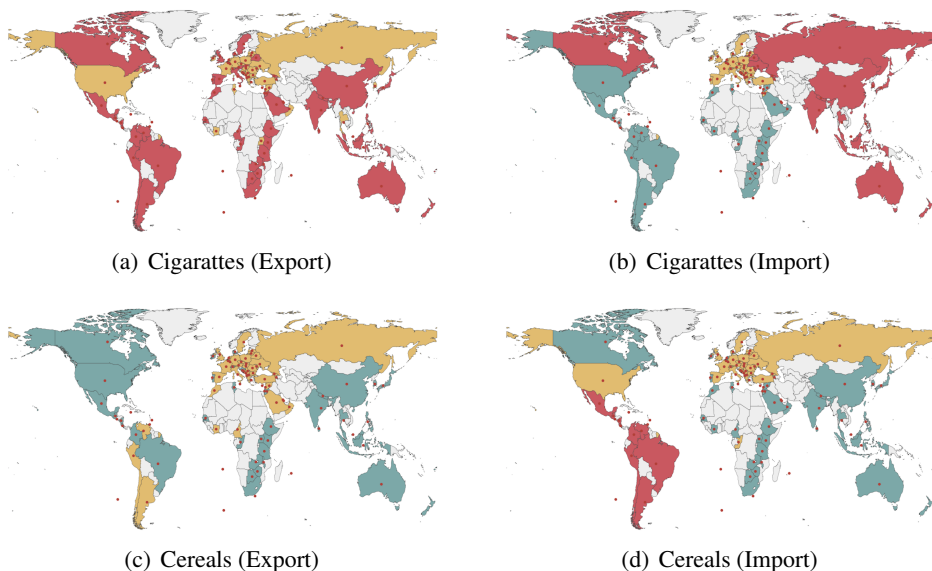


Figure 7: The World Maps display: (a) cigarette export clustering, (b) cigarette import clustering, (c) cereal export clustering, and (d) cereal import clustering.

Figures 5 and 6 showcase the original network’s heatmap alongside the reordered block cosine similarity matrix obtained by the DOM algorithm. The block cosine similarity matrix reveals distinct block patterns for exporting and importing countries, effectively demonstrating the TNPM’s capacity to delineate network communities- export countries split into two groups and import countries into three, respectively.

Figure 7 displays country clusters with identical colors marking the same cluster and grey areas indicating excluded countries. Figure 7 (b) showcases country clusters in cigarette imports, revealing significant regional trade patterns. Specifically, European nations emerge as a major cluster of tobacco importers, while another cluster includes China, India, Indonesia, and other Southeast Asian and Oceanian countries, mainly sourcing tobacco from Brazil, the United States, Canada, and Argentina. A distinct cluster comprises the United States, and certain South American, and African countries, highlighting the strategic advantages of regional trading, such as lower transportation costs and quicker delivery times.

6.2 MovieLens 100K Dataset

The MovieLens 100K data set, documented by Harper and Konstan (2015), is collected by the GroupLens Research of the MovieLens website (movielens.umn.edu), and is accessible at <https://grouplens.org/datasets/movielens/100k>. This data set contains 10,000 ratings from 943 users across 1682 movies, leading to the construction of a 943×1682 rating matrix A , where each element $A_{i,j}$ denotes the rating from 1 to 5 given by user i to movie j . The movies are categorized into 19 genres, including “Adventure,” “Action,” and “Animation,” among others, with 833 movies categorized in a single genre and the rest in multiple genres.

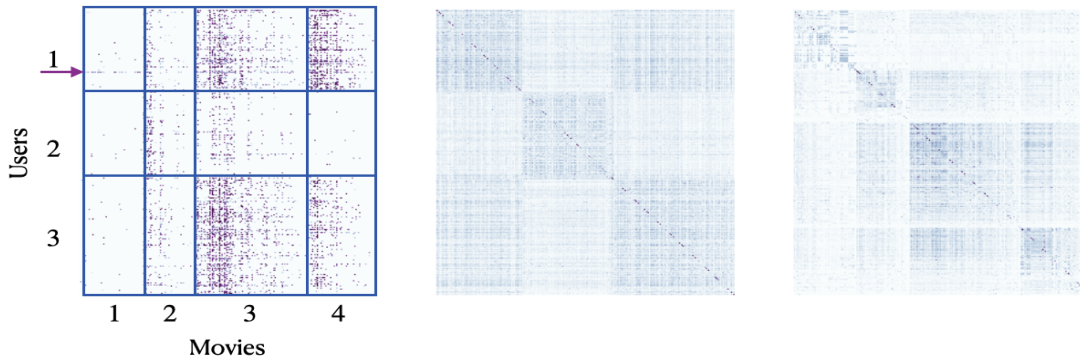


Figure 8: The heatmap of the MovieLens matrix A (left) and the rearranged block cosine similarity matrix for rows (middle) and columns (right).

We employ the proposed algorithm to bicluster the MovieLens 100K data set. Following the parameters set forth in Flynn and Perry (2020) and Zhao et al. (2024), we establish $K = 3$ for user clusters and $L = 4$ for movie clusters. We present the TSDC’s results here and leave the DOM’s in Appendix D.2.

Figure 8 displays the data matrix heatmap and block cosine similarity matrix, with nodes organized by TSDC algorithm-detected community assignments. The left panel reveals that nodes within the same user cluster exhibit diverse patterns of node popularity across different movie clusters. For instance, in user cluster 1, one individual shows a notable preference for cluster 1 movies, whereas the rest of user cluster 1 members provide significantly fewer ratings for these films. Furthermore, our results reveal distinct consumer behavior patterns. Significantly, users in cluster 3 predominantly review movies within cluster 3, while movies in cluster 4 are primarily reviewed by users in cluster 1. The middle and right panels clearly illustrate the distinct block structures and emphasize the suitability of the TNPM for modeling the data set.

We investigate the association between estimated movie clusters and actual movie categories provided in the MovieLens data set. The direct comparison faced challenges due to the vast array of movie categories and their overlaps. To address this, we filtered the data set to 833 films, each in a unique category. We perform the chi-squared test of independence on the contingency tables and obtain p-values of 4.39×10^{-8} and 3.003×10^{-11} for the clusters estimated by the DOM and TSDC algorithms, respectively. These p-values are smaller than the reported testing p-values in Flynn and Perry (2020) (0.0415) and Zhao et al. (2024) (2.656×10^{-7}), indicating a stronger association between the algorithm-predicted clusters and the true movie categories.

References

- Arash A Amini, Aiyou Chen, Peter J Bickel, and Elizaveta Levina. Pseudo-likelihood methods for community detection in large sparse networks. *The Annals of Statistics*, 41(4):2097–2122, 2013.
- Peter J Bickel and Aiyou Chen. A nonparametric view of network models and newman–girvan and other modularities. *Proceedings of the National Academy of Sciences*, 106(50):21068–21073, 2009.
- Genís Calderer and Marieke L Kuijjer. Community detection in large-scale bipartite biological networks. *Frontiers in Genetics*, page 520, 2021.
- Manlio De Domenico, Vincenzo Nicosia, Alexandre Arenas, and Vito Latora. Structural reducibility of multilayer networks. *Nature communications*, 6(1):1–9, 2015.
- Cheryl Flynn and Patrick Perry. Profile likelihood biclustering. *Electronic Journal of Statistics*, 14(1):731–768, 2020.
- F Maxwell Harper and Joseph A Konstan. The movielens datasets: History and context. *Acm transactions on interactive intelligent systems (tiis)*, 5(4):1–19, 2015.
- Pengsheng Ji and Jiashun Jin. Coauthorship and citation networks for statisticians. *The Annals of Applied Statistics*, 10(4):1779–1812, 2016.
- Bing-Yi Jing, Ting Li, Zhongyuan Lyu, and Dong Xia. Community detection on mixture multilayer networks via regularized tensor decomposition. *The Annals of Statistics*, 49(6):3181–3205, 2021.
- Bingyi Jing, Ting Li, Ningchen Ying, and Xianshi Yu. Community detection in sparse networks using the symmetrized laplacian inverse matrix (slim). *Statistica Sinica*, 32(1):1, 2022.
- Andrea Lancichinetti, Santo Fortunato, and János Kertész. Detecting the overlapping and hierarchical community structure in complex networks. *New journal of physics*, 11(3):033015, 2009.
- Ting Li, Jianchang Hu, Shiyong Wang, and Heping Zhang. Super-variants identification for brain connectivity. *Human brain mapping*, 42(5):1304–1312, 2021.
- Majid Noroozi, Marianna Pensky, and Ramchandra Rimal. Sparse popularity adjusted stochastic block model. *The Journal of Machine Learning Research*, 22(1):8671–8706, 2021a.
- Majid Noroozi, Ramchandra Rimal, and Marianna Pensky. Estimation and clustering in popularity adjusted block model. *Journal of the Royal Statistical Society Series B: Statistical Methodology*, 83(2):293–317, 2021b.
- Karl Rohe, Tai Qin, and Bin Yu. Co-clustering directed graphs to discover asymmetries and directional communities. *Proceedings of the National Academy of Sciences*, 113(45):12679–12684, 2016.
- Srijan Sengupta and Yuguo Chen. A block model for node popularity in networks with community structure. *Journal of the Royal Statistical Society: Series B (Statistical Methodology)*, 80(2):365–386, 2018.

- Jiangzhou Wang, Jingfei Zhang, Binghui Liu, Ji Zhu, and Jianhua Guo. Fast network community detection with profile-pseudo likelihood methods. *Journal of the American Statistical Association*, 118(542):1359–1372, 2023.
- Junhui Wang. Consistent selection of the number of clusters via crossvalidation. *Biometrika*, 97(4): 893–904, 2010.
- Zhe Wang, Yingbin Liang, and Pengsheng Ji. Spectral algorithms for community detection in directed networks. *The Journal of Machine Learning Research*, 21(1):6101–6145, 2020.
- Ling Wu, Qishan Zhang, Chi-Hua Chen, Kun Guo, and Deqin Wang. Deep learning techniques for community detection in social networks. *IEEE Access*, 8:96016–96026, 2020.
- Jingnan Zhang, Xin He, and Junhui Wang. Directed community detection with network embedding. *Journal of the American Statistical Association*, pages 1–11, 2021.
- Yunpeng Zhao, Elizaveta Levina, and Ji Zhu. Consistency of community detection in networks under degree-corrected stochastic block models. *The Annals of Statistics*, 40(4):2266–2292, 2012.
- Yunpeng Zhao, Ning Hao, and Ji Zhu. Variational estimators of the degree-corrected latent block model for bipartite networks. *Journal of Machine Learning Research*, 25(150):1–42, 2024.
- Zhixin Zhou and Arash A Amini. Analysis of spectral clustering algorithms for community detection: the general bipartite setting. *The Journal of Machine Learning Research*, 20(1):1774–1820, 2019.
- Zhixin Zhou and Arash A Amini. Optimal bipartite network clustering. *The Journal of Machine Learning Research*, 21(1):1460–1527, 2020.